ATTENUATION OF LONG PERIOD STRONG GROUND MOTIONS

Norman A,. Abrahamson
Castro Valley, CA

Walter J. Silva
Pacific Engineering and Analysis
El Cerrito, CA

ABSTRACT

Empirical strong motion recordings from large magnitude (M≥6) events are reprocessed using procedures that emphasize preserving the long period motions and determining the reliable period range for each recording. An empirical attenuation relationship for 5% damped response spectral values is derived for the period range 1-20 second and rupture distances of 1 to 100 km. Numerical simulations are used to guide the selection of the functional form of the regression equation and the extension of the attenuation relations up to a period of 20 seconds.

INTRODUCTION

For seismic isolation systems, the critical frequency band for seismic ground motions is shifted from short periods to low frequencies. This has lead to increased interest in attenuation relations for long period ground motions. The major difficulty in estimating long period spectral attenuation relations from empirical data is that much of the processed data may be unreliable at periods greater than several seconds. To address this problem, strong motion recordings from large magnitude earthquakes are reprocessed using a procedure that is directed at recovering the long period motion. In addition, a new procedure for evaluating the reliable long period range for strong motions based on the Fourier phase spectrum is developed and applied.

Based on our analysis, at periods greater than 10 seconds, very few of the accelerograms contain energy above the noise level. We used numerical modeling to guide the extension of the attenuation relations to periods up to 20 seconds. This paper describes the long period attenuation relations derived using recordings from large magnitude events (M≥6).

DATA BASE

The strong motion data base for this study consists of 201 recordings from 18 events with magnitude greater or equal to 6.0 and distance less than 100 km. Distance is defined as closest distance to the rupture zone and magnitude is moment magnitude. The events used in this study are listed in Table 1. The geometric average of the horizontal components is used.

Based upon site response analyses using broad categories and generic site profiles (Silva, 1991), the sites were initially classified as rock, shallow soil (<250 ft), intermediate depth soil (250-1000 ft), deep soil (>1000 ft), and alluvium of unknown depth. There are insufficient recordings in the shallow and intermediate categories to evaluate these categories separately. Therefore, we combined the data into two groups: soil < 250 ft and soil > 250 ft. The "alluvium of unknown depth" was put into the soil > 250 ft group. The distribution of recordings in magnitude and distance is shown in Figure 1. The Nahanni earthquake recordings were only used for the absolute spectral levels and not for peak acceleration because they are more representative of Eastern U. S. rock conditions than Western U. S. rock site conditions.

CORRECTION PROCEDURE

In order to extend the strong motion data base to the longest periods as possible, all of the records were reprocessed. The correction procedure includes both a high-pass filter in the frequency domain and a polynomial baseline correction in the time domain (Gaizer (1979). The details of the correction procedure are given in Silva and Abrahamson (1993).

The judgement whether long period motion for a given record is realistic depends on the consistency of the amplitudes and timing of the long period energy with that of the higher frequency motion. One way to quantify the consistency of the timing of the long period motions is by examining the phase spectrum. The phase spectrum controls the timing and shape of the waveform. Seismic ground motion are expected to have a consistent phase structure at long periods whereas noise will have random phase.

TABLE 1. STRONG MOTION DATA BASE

Event	M	R	S	I	D	A	Total
1940 El Centro	7.1				1		1
1952 Kern County	7.4				4	1	5
1966 Parkfield	6.1	2			4		6
1968 Borrego Mtn.	6.6				1		1
1971 San Fernando	6.6	10	1	1	3	1	16
1976 Gazli	6.8				1		1
1976 Friuli	6.2	1	1			2	4
1978 Tabas	7.4	2					2
1978 Santa Barbara	6.0	1			1		2
1979 Imperial Valley	6.5	2			21	8	31
1980 Mexicali Valley	6.4	1				4	5
1983 Coalinga	6.5	21	17		1	4	43
1984 Morgan Hill	6.2	6	2	1	7	6	22
1985 Nahanni	6.8	3					3
1987 Superstition Hills A	6.2				1		1
1987 Superstition Hills B	6.6				2		2
1988 Spitak	7.0	1					1
1989 Loma Prieta	7.0	28	4	3	15	5	55
Total		78	25	5	62	31	201

R=rock, S=shallow soil, I=intermediate depth soil, D=deep soil, A=alluvium of unknown depth.

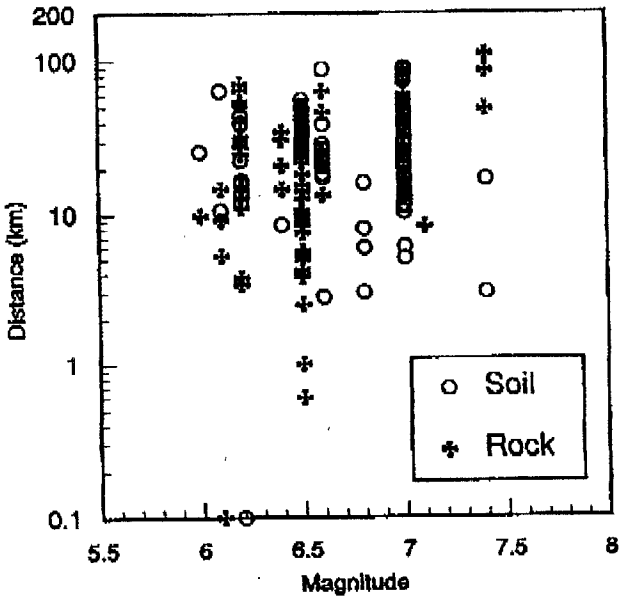

FIGURE 1. DISTANCE AND MAGNITUDE DISTRIBUTION OF THE DATA BASE.

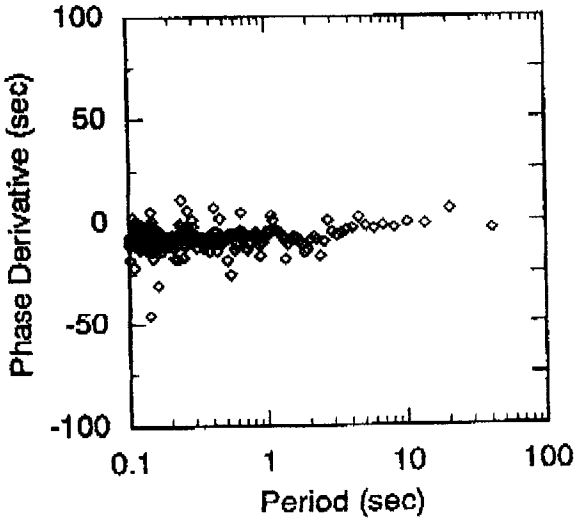

FIGURE 2A. SAMPLE ANALYTICAL PHASE DERIVATIVE. IN THIS CASE, THE PHASE DERIVATIVE IS WELL BEHAVED FOR PERIODS UP TO 20 SECONDS.

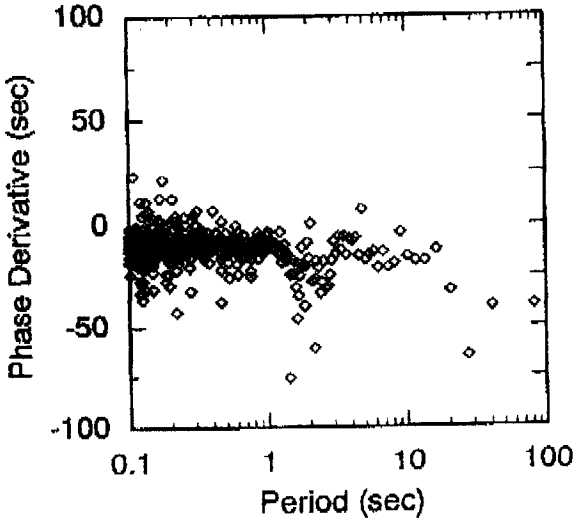

FIGURE 2B. SAMPLE ANALYTICAL PHASE DERIVATIVE. IN THIS CASE, THE PHASE DERIVATIVE BECOMES MORE RANDOM AT A PERIOD OF ABOUT 1.5 SECONDS.

Specifically, we examine the analytical derivative of the phase with respect to frequency (Tribolet, 1977). Examples of the phase derivative are shown in Figures 2a and b. Figure 2a shows a case where the phase derivative is well behaved to periods of 20 seconds. In contrast, Figure 2b shows a case where the phase derivative becomes much more random at a period of about 1.5 seconds. The final corrected acceleration time histories are evaluated for long period noise contamination by examining the analytic phase derivative.

The high-pass filter corner frequencies used in the correction procedure and the behavior of the phase derivative are used to limit the longest reliable period for each record. The response spectral values are only used in the regression for frequencies that are greater than 1.25 times the high-pass filter corner frequency. Also, response spectra values are only used for periods less than the shortest period at which the phase derivative is not well behaved. The size of the data base for each period is listed in Table 2. These restrictions on the data set will tend to bias the regression to larger spectral values because the larger motions will be above the noise level more often than smaller motions. In this study, we do not try to correct for this bias, but simply note that this conservatism is inherent to our procedure.

REGRESSION ANALYSES

The regression analyses use the random effects model following the algorithm of Abrahamson and Youngs (1992). This model explicitly accounts for the correlation between recordings from the same earthquake. It handles uneven sampling of the earthquakes in a statistically optimal manner. This method partitions the variance into inter-event (τ^2) and intra-event (σ^2) terms.

The regression is performed for peak acceleration (pga) and response spectral values. The regression for response spectral values uses the spectral shape (Sa/pga) because it is more stable than the absolute spectral values. The final response spectral attenuation is found by combining the spectra shape model with the pga model. The standard error of the spectral attenuation relation is computed using the absolute spectral values.

Peak Acceleration

The horizontal peak acceleration on rock is modeled by:

$$\ln pga_{rock}(g) = \theta_1 + \theta_2 M + \theta_3 \ln(r+\exp(\theta_4+\theta_5 M)) + \theta_{11} F_1 \quad (1)$$

and the horizontal peak acceleration on soil is modeled by

$$\ln pga_{rock}(g) = \theta_6 + \theta_7 M + \theta_8 \ln(r+\exp(\theta_9+\theta_{10} M)) + \theta_{11} F_1 \quad (2)$$

where r is the closest distance to the rupture zone in km, M is moment magnitude, and F_1 is the fault type (F_1=1 for reverse and zero for strike-slip or normal).

The estimated coefficients for average horizontal pga are listed in Table 3. The resulting pga attenuation relations are shown in Figure 3.

Spectral Shape

The functional form for the average horizontal spectral shape was guided by results from numerical simulations and previous empirical studies. Depending on the assumptions regarding the seismic source parameter values, numerical simulations suggest that strike-slip events maybe more likely to show near-field directivity effects at long periods than dip-slip events. The functional form is selected so that it can accommodate this effect. The normalized spectrum model is given by

$$\ln(Sa/pga)_{soil} = c_1 + c_2 (8.5-M)^{c8} + c_6 r + c_5 (1-\tanh((r-c_9)/c_{10})) (1-F_2) \quad (3)$$

and

$$\ln(Sa/pga)_{rock} = c_3 + c_4 (8.5-M)^{c8} + c_7 r + c_5 (1-\tanh((r-c_9)/c_{10})) (1-F_2) \quad (4)$$

where F_2=0 for strike-slip events and F_2=1 for dip-slip events. The last term accommodates a near-field effect for strike-slip events.

The analysis of the data showed that the near-field effect for strike-slip events decreased for events with magnitude less than 6.5.

TABLE 2. SIZE OF RELIABLE DATA BASE FOR DIFFERENT PERIODS

Period (sec)	Events	Records
0.0	18	201
1.0	18	200
1.5	18	197
2.0	18	180
3.0	18	173
4.0	17	161
5.0	12	85
7.5	11	77
10.0	6	31
15.0	5	29
20.0	1	22

TABLE 3. AVERAGE HORIZONTAL PGA COEFFICIENTS

θ_1	-4.364
θ_2	1.016
θ_3	-1.285
θ_4	-3.34
θ_5	0.79
θ_6	-8.698
θ_7	1.654
θ_8	-1.166
θ_9	-6.80
θ_{10}	1.40
θ_{11}	0.17
σ	0.44
τ	0.00
σ_{Total}	0.44

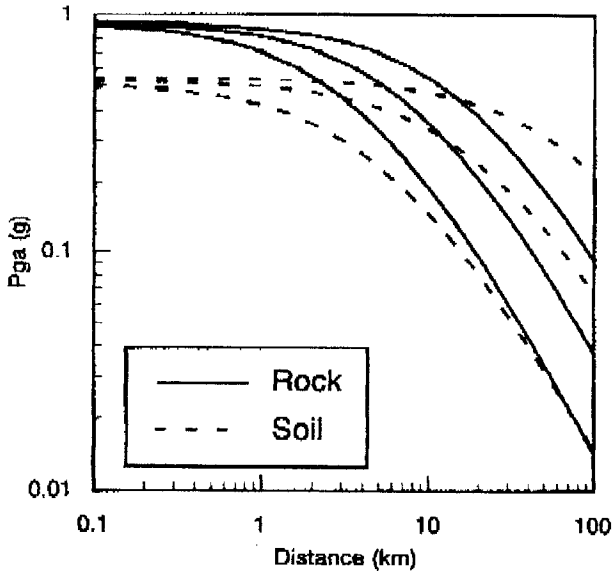

FIGURE 3. STRIKE-SLIP HORIZONTAL PEAK ACCELERATION ATTENUATION RELATION FOR MAGNITUDES 6, 7, AND 8. THE SOLID CURVES ARE FOR ROCK SITES AND THE DASHED CURVES ARE FOR SOIL SITES.

Therefore, the functional form was modified for events between magnitude 6 and 6.5 to taper out the near-field effect for strike-slip events. For 6.0≤M<6.5, the normalized spectrum is modeled by

$$\ln(Sa/pga)_{soil} = c_1 + c_2 (8.5-M)^{c8} + c_6 r + 2(M-6)\, c_5 (1-\tanh((r-c_9)/c_{10}))\,(1-F_2) \quad (5)$$

$$\ln(Sa/pga)_{rock} = c_3 + c_4 (8.5-M)^{c8} + c_7 r + 2(M-6)\, c_5 (1-\tanh((r-c_9)/c_{10}))\,(1-F_2) \quad (6)$$

The coefficients computed for the rock/shallow soil and deep soil site conditions are listed in Table 4. The near-field term, c_5, corresponds to up to a 30% difference in long period spectral shape at short distances between strike-slip and dip-slip events. The empirical data could only be used for periods up to 7.5 seconds because there were not enough records that were reliable for periods of 10 seconds or greater to yield a stable regression result (Table 2). Based on numerical simulations, the response spectrum is approximately flat to spectral displacement at periods greater than 8 seconds for magnitudes less than 7.5. Therefore, the spectral attenuation relations were extended to 20 seconds assuming constant spectral displacement. For magnitudes larger than 7.5, this extension may not be appropriate.

The standard errors of the absolute spectral acceleration based on the combined pga and spectral shape attenuation relations are listed in Table 5. In contrast to the pga standard error, the long period spectral standard errors have a significant inter-event component (τ), generally about the same size as the intra-event component (σ).

TABLE 4. COEFFICIENTS FOR HORIZNTAL SPECTRAL SHAPE

per	c_1	c_2	c_3	c_4	c_5	c_6	c_7	c_8	c_9	c_{10}
1.0	0.5331	-0.08	0.0259	-0.103	0.13	0.0025	0.009	2.5	10	3
1.5	0.1004	-0.08	-0.4264	-0.105	0.13	0.0025	0.009	2.5	10	3
2.0	-0.2137	-0.08	-0.7692	-0.118	0.13	0.0025	0.009	2.5	10	3
3.0	-0.8873	-0.08	-1.3057	-0.14	0.13	0.0025	0.009	2.5	10	3
4.0	-1.3105	-0.11	-1.6072	-0.17	0.13	0.0025	0.009	2.5	10	3
5.0	-1.4497	-0.15	-1.8304	-0.21	0.13	0.0025	0.009	2.5	10	3
7.5	-2.2523	-0.15	-2.6086	-0.21	0.13	0.0025	0.009	2.5	10	3
10.0	-2.8235	-0.15	-3.1675	-0.21	0.13	0.0025	0.009	2.5	10	3
15.0	-3.6344	-0.15	-3.9785	-0.21	0.13	0.0025	0.009	2.5	10	3
20.0	-4.2098	-0.15	-4.5538	-0.21	0.13	0.0025	0.009	2.5	10	3

TABLE 5. STANDARD ERRORS FOR HORIZONTAL SA

Per (sec)	σ	τ	σ_{Total}
1.0	0.53	0.49	0.72
1.5	0.50	0.49	0.70
2.0	0.48	0.43	0.64
3.0	0.51	0.44	0.67
4.0	0.48	0.50	0.69
5.0	0.52	0.47	0.70
7.5	0.58	0.43	0.72
10.0			0.72*
15.0			0.72*
20.0			0.72*

* Assumed Value

At periods greater than 7.5 seconds, the total standard error is assumed to be the same as the 7.5 second level.

The resulting spectral displacement attenuation relation for strike-slip events is plotted as a function of period in Figures 4a and b for distance of 1 and 10 km, respectively. A 1 km, the difference between soil and rock is small due to the larger pga for rock at short distances (Fig. 3). At 10 km, the soil spectral displacement becomes significantly larger than the rock spectral displacement. The attenuation relations are shown as a function of distance for a period of 2 seconds in Figure 5.

The recent Lander Earthquake (M~7.5) was recorded at the Lucerne station operated by Southern California Edison. It was located about 1.8 km from the fault rupture on rock. A final corrected version of this record is not yet available. A preliminary corrected record was produced using the same baseline correction procedure that was used to correct the data for this study. The resulting geometric average horizontal spectral displacement is compared to the attenuation relation in Figure 6. The attenuation relation overpredicts the Lucerne recording. The larger horizontal component of the Lucerne record is up to a factor of 2 larger than the geometric average. Large differences between the two horizontal components have been observed for other recordings at short distances (Sadigh et al., 1993; Somerville and Graves, 1993).

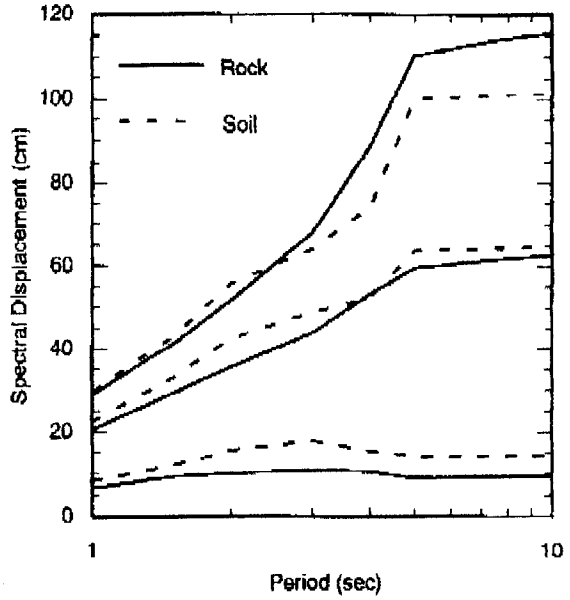

FIGURE 4A. MEDIAN 5% DAMPED SPECTRAL DISPLACEMENT FOR STRIKE-SLIP EVENTS WITH MAGNITUDES 6, 7, AND 8 AT A DISTANCE OF 1 KM. THE SOLID LINES ARE FOR ROCK AND THE DASHED LINES ARE FOR SOIL.

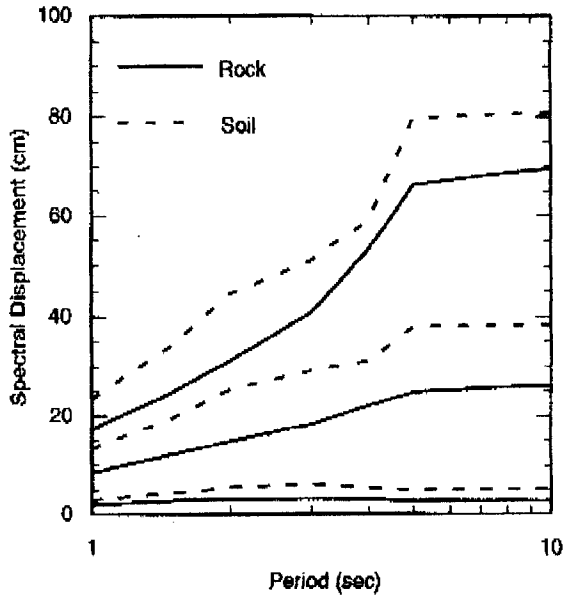

FIGURE 4B. MEDIAN 5% DAMPED SPECTRAL DISPLACEMENT FOR STRIKE-SLIP EVENTS WITH MAGNITUDES 6, 7, AND 8 AT A DISTANCE OF 10 KM. THE SOLID LINES ARE FOR ROCK AND THE DASHED LINES ARE FOR SOIL.

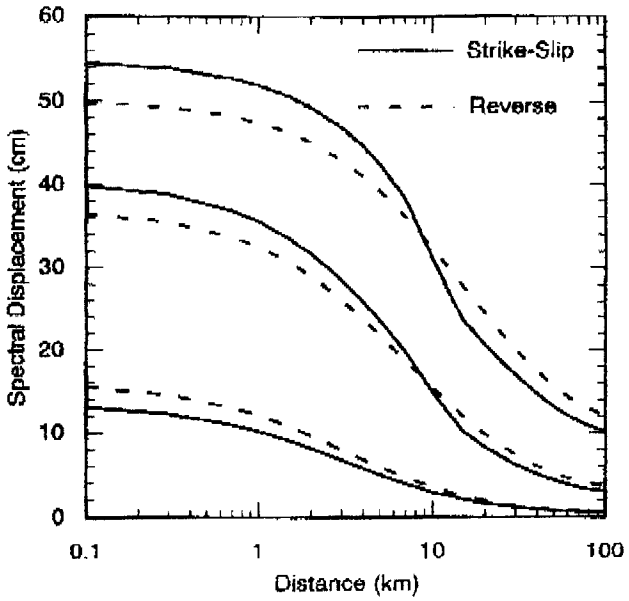

FIGURE 5. MEDIAN 5% DAMPED SPECTRAL DISPLACEMENT AT A PERIOD OF 2 SECONDS ON ROCK FOR MAGNITUDES 6, 7, AND 8.

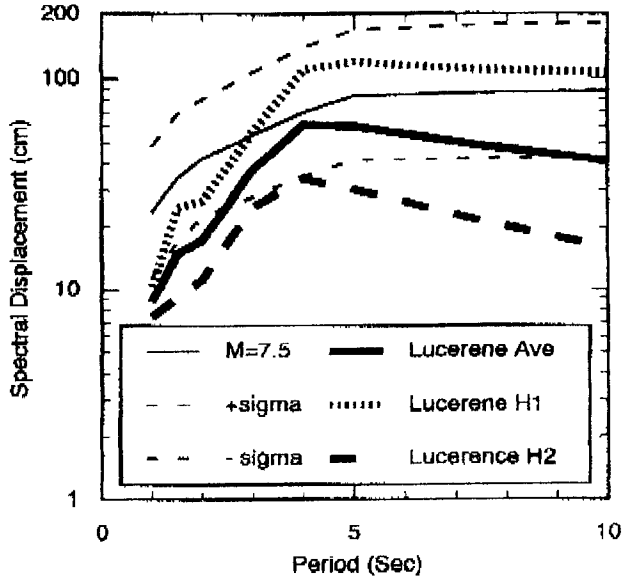

FIGURE 6. COMPARISON OF THE PREDICTED AVERAGE HORIZONTAL SPECTRUM FOR A M=7.5 STRIKE-SLIP EVENT ON ROCK (THIN LINES) WITH A PRELIMINARY ESTIMATE OF THE HORIZONTAL SPECTRUM FROM THE LUCERNE RECORDING OF THE 1992 LANDERS EARTHQUAKE (HEAVY LINES). THE AVERAGE HORIZONTAL COMPNENT IS SHOWN BY THE SOLID LINE AND THE INDIVIDUAL HORIZONTAL COMPONENTS ARE SHOWN BY THE DASHED AND DOTTED LINES.

ACKNOWLEDEMENT

This study was supported by the Strong Motion Instrumentation Program of the California Division of Mines and Geology.

REFERENCES

Abrahamson, N.A. and R.P. Youngs (1992). A stable algorithm for regression analyses using the random effects model, Bull. Seism. Soc. Am., 505-510.

Graizer, V. U. (1979). Determination of the true ground displacement by using strong motion records, Physics Solid Earth, Ins. Acad. Sc., USSR, English Ed.

Sadigh, K., C. Y. Chang, N. A. Abrahamson, S. J. Chiou, and M. S. Power (1993). Specification of long-period ground motions: Updated attenuation relationships for rock site conditions and adjustment factors for near-fault effects, ATC-17-1 Seminar on Seismic Isolation, Passive Energy Dissipation, and Active Control, Vol I, 59-70, San Francisco, March 11-12, 1993.

Silva, W. (1991). Site geometry and global characteristics, Proc. NSF/EPRI Workshop on Dynamic Soil Properties and Site Characterization, Palo Alto, CA.

Silva, W. and N. A. Abrahamson (1993). Quantification of long period strong motion ground motion attenuation for engineering design, Calif. Div. Mines. Geol., SMIP Research Program, Final Report.

Somerville, P. G. and R. Graves (1993). Conditions that give rise to unusally large long period ground motion, ATC-17-1 Seminar on Seismic Isolation, Passive Energy Dissipation, and Active Control, Vol I, 83-94, San Francisco, March 11-12, 1993.

Tribolet, S.M. (1977). A new phase unwrapping algorithm, IEEE Trans, ASSP-25, 170-177.